

Application of triple-layer remote phosphor configuration results in the color quality and luminous efficiency enhancement of WLEDs

Thuc Minh Bui¹, Phan Xuan Le², Dinh Hoang Bach³, Nguyen Doan Quoc Anh^{*4}

¹Faculty of Electrical and Electronics Engineering, Nha Trang University, Nha Trang City, Vietnam

²National Key Laboratory of Digital Control and System Engineering, Ho Chi Minh City, Vietnam

³Faculty of Electrical and Electronics Engineering, Ton Duc Thang University, Ho Chi Minh City, Vietnam

⁴Power System Optimization Research Group, Faculty of Electrical and Electronics Engineering, Ton Duc Thang University, Ho Chi Minh City, Vietnam

*Corresponding author, e-mail: nguyendoanquocanh@tdtu.edu.vn

Abstract

This study proposed the triple-layer remote phosphor (TRP) structure to enhance the color quality and the emitted luminous flux of white LEDs (WLEDs). The TRP structure consists of three different phosphor layers that are arranged as follows: the yellow YAG:Ce³⁺ phosphor at the bottom, the red phosphor layer CaMgSi₂O₆:Eu²⁺,Mn²⁺ at the top and the green Ba₂Li₂Si₂O₇:Sr²⁺,Mn²⁺ phosphor between these two ones. The aim to use the red CaMgSi₂O₆:Eu²⁺,Mn²⁺ phosphor is to control the red light component so that the color rendering index (CRI) could be increased. While the green Ba₂Li₂Si₂O₇:Sr²⁺,Mn²⁺ phosphor is applied to manage the green light component, leading to the rise in luminous efficacy (LE) of WLEDs. Moreover, when the concentrations of these two phosphors are raised, that of the yellow phosphor YAG:Ce³⁺ has to be decreased to remain the average correlated color temperatures (ACTTs) in a range from 6000 K to 8500 K. Furthermore, not only the CRI and LE but the color quality scale (CQS) is also analyzed by controlling the two green and red phosphor concentrations. The researched results show that the higher the concentration of CaMgSi₂O₆:Eu²⁺,Mn²⁺, the more enhancements in the CRI will be made. In contrast, when the Ba₂Li₂Si₂O₇:Sr²⁺,Mn²⁺ concentration increases, the CRI significantly decreases. Meanwhile, CQS is likely to considerably rise in a concentration range from 10% to 14% of CaMgSi₂O₆:Eu²⁺,Mn²⁺, regardless of the presence of Ba₂Li₂Si₂O₇:Sr²⁺,Mn²⁺ concentration. Especially, in parallel with the improvement of CRI and CQS, the LE could be also increased by more than 40% due to the decline in back-scattering lights and the green lights supplement. From these details, the results of this study are valuable references for manufacturers to achieve the goals of enhancing color quality and luminous efficiency of WLEDs.

Keywords: color quality, luminous flux, remote phosphor package, triple-layer structure, WLEDs

Copyright © 2019 Universitas Ahmad Dahlan. All rights reserved.

1. Introduction

As the demands of lighting market have been increasing rapidly, phosphor-converted white light-emitting diodes (WLEDs) has become a potential light source that is able to meet those demands, due to their stand out features, including small size, high energy efficiency, low cost, and color stability [1-4]. To generate high-quality lights, WLEDs are manufactured by applying the combination between the blue light from a blue chip and the yellow light from phosphor which is also known as the principle of complementary colors [5-8]. Though the usage of WLEDs in solid-state-lighting is promising, this light source must be enhanced in terms of its luminous efficiency [9, 10]. In general, white light can be produced by applying many methods, but freely dispersed coating is the most common one. Specifically, in this method, the phosphor package of WLEDs is covered with a mixture of transparent encapsulated resin and phosphor powder. By using this approach, it is able to get the thickness of the phosphor layer controlled and also significantly reduce the production cost, yet this method is not efficient in fabricating high-quality WLEDs [7]. Hence, there is an alternative method which is expected to bring better results, the conformal coating method. With this method, the color uniformity can be achieved, leading to angular homogeneity of correlated color temperature (CCT) [11-13]. However, the conformal phosphor structure causes luminous efficiency to be decreased due to the backscattering effect.

Besides, the idea of separating the chip and the phosphor layer of remote phosphor structures has been mentioned in many previous studies [14, 15]. In specific, this concept can be described as the two following structures. The first one is the internal reflection structure which could enhance light extraction by using a polymer hemispherical shell lens and interior phosphor coating, and this is considered as an approach contributing in increasing extraction efficiency [16-18]. The second one is the air-gap embedded structure which could get luminous efficiency improved due to its ability reflect downward light [19].

However, to achieve higher luminous efficiency, it is necessary to focus on not only the structure of the package but also the concentration of phosphor. The researches have demonstrated that as the phosphor concentration is in an increase, it has resulted in the rising loss of the re-absorption in the phosphor layer. Thus, the quality of luminous efficiency of the device has been presented in a downward trend, especially at lower CCTs [20]. Therefore, to get the luminous efficiency lifted up, the emission of blue and yellow rays needs to be promoted, and the loss of light caused by backscattering and reflection must be reduced.

The triple-layer remote phosphor structure of WLEDs with average correlated temperature colors from 6000 K to 8500 K is recommended in this article. There are three phosphor layers comprising the TRP, including the green $\text{Ba}_2\text{Li}_2\text{Si}_2\text{O}_7:\text{Sn}^{2+},\text{Mn}^{2+}$ phosphor layer placed between the two layers of yellow $\text{YAG}:\text{Ce}^{3+}$ and red $\text{CaMgSi}_2\text{O}_6:\text{Eu}^{2+},\text{Mn}^{2+}$ phosphor. The green phosphor layer is used to enhance the green light component resulting in better luminous efficiency. While the red-light component is supplemented by the red phosphor layer leading to the enhancement in the color quality of WLEDs. The research results have shown that when the three colors yellow, green and red are balanced, the color quality can reach the highest value, while the luminous flux of WLEDs decreases insignificantly.

2. Research Method

2.1. Preparation of Phosphor Materials

The first idea of this research is manipulating the green phosphor layer of $\text{Ba}_2\text{Li}_2\text{Si}_2\text{O}_7:\text{Sn}^{2+},\text{Mn}^{2+}$ to increase the green light component in WLEDs, resulting in better luminous flux. While, in the second idea, the red $\text{CaMgSi}_2\text{O}_6:\text{Eu}^{2+},\text{Mn}^{2+}$ phosphor layer is applied to grow the number of red light components so that the CRI and CQS could be also lifted. The article also demonstrates in details the chemical composition of these phosphor materials which affect the optical characteristics of WLEDs. The composition of red $\text{CaMgSi}_2\text{O}_6:\text{Eu}^{2+},\text{Mn}^{2+}$ phosphor is illustrated in Table 1.

Table 1. Composition of Red-Emitting $\text{CaMgSi}_2\text{O}_6:\text{Eu}^{2+},\text{Mn}^{2+}$ Phosphor

| Ingredient | Mole (%) | By weight (g) | Molar mass (g/mol) | Mole (mol) | Ions | Mole (mol) | Mole (%) |
|-------------------------|----------|---------------|--------------------|------------|------------------|------------|----------|
| CaO | 45.69 | 150 | 56.0774 | 2.67 | Ca^{2+} | 2.67 | 0.19 |
| MgO | 16.95 | 40 | 40.304 | 0.99 | Mg^{2+} | 0.99 | 0.07 |
| SiO_2 | 35.82 | 126 | 60.08 | 2.10 | Si^{4+} | 2.10 | 0.15 |
| Eu_2O_3 | 0.17 | 3.5 | 351.926 | 0.01 | O^{2-} | 8.13 | 0.58 |
| MnCO_3 | 1.37 | 9.2 | 114.9469 | 0.08 | Eu^{2+} | 0.02 | 0.0014 |
| NH_4Cl | -- | 5.4 | 53.49 | -- | Mn^{2+} | 0.08 | 0.0057 |

$\text{CaMgSi}_2\text{O}_6:\text{Eu}^{2+},\text{Mn}^{2+}$ phosphor is produced through a process of six steps, including mixing, double drying, firing twice and washing. Moreover, these steps have to be followed in a strict order to get the best result as follows. Initially, the materials are slurried in in methanol to create a mixture. In this step, the way to soak with a few cubic centimeters water is the key that should be focused on. Next, the mixture will be dried in air, before being fired in capped quartz tubes with N_2 at 1000°C for an hour. After the firing process, this mixture will be powderized, and then re-fired in capped quartz tubes with CO at the temperature of 1150°C within 1 hour. Finally, the product will be washed in water several times. When the product dry, we will get the complete $\text{CaMgSi}_2\text{O}_6:\text{Eu}^{2+},\text{Mn}^{2+}$.

In Table 2, the composition of green $\text{Ba}_2\text{Li}_2\text{Si}_2\text{O}_7:\text{Sn}^{2+},\text{Mn}^{2+}$ phosphor is presented. The producing process of the green $\text{Ba}_2\text{Li}_2\text{Si}_2\text{O}_7:\text{Sn}^{2+},\text{Mn}^{2+}$ phosphor from the ingredients in Table 2 is presented as the following steps. Initially, mixing the materials of BaCO_3 , Li_2CO_3 and

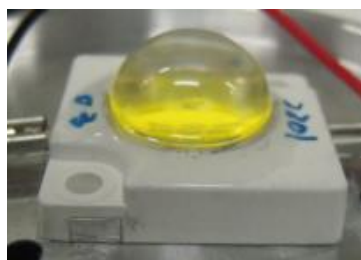
SiO₂ together by dry grinding or milling. After that, the obtained mixture will be fired in open boats with H₂ at 850°C for 1 hour. Next, adding SnO, MnCO₃ and NH₄Br to the mixture. Then putting the whole mixture into methanol to make a slurry and stirring until it becomes uniform. Then, this mixture will be powderized after being dried in air. In the next steps, the powder will be put into capped quartz tubes and fired with N₂ at 850°C within an hour. After the second firing, the materials will be powderized again, and then, they will be fired once more time in open quartz boats with CO at the same temperature of 850°C for approximately 16 hours (overnight). Next, the mixture will go through another powderizing. Finally, the attained materials will be stored in a well-closed container.

Table 2. Composition of Green-emitting Ba₂Li₂Si₂O₇:Sn²⁺,Mn²⁺ Phosphor

| Ingredient | Mole (%) | By weight (g) | Molar mass (g/mol) | Mole (mol) | Ions | Mole (mol) | Mole (%) |
|---------------------------------|----------|---------------|--------------------|------------|------------------|------------|----------|
| BaCO ₃ | 25.04 | 185 | 197.34 | 0.94 | Ba ²⁺ | 0.94 | 0.082 |
| Li ₂ CO ₃ | 14.82 | 41 | 73.891 | 0.55 | Li ⁺ | 1.11 | 0.097 |
| SiO ₂ | 29.34 | 66 | 60.08 | 1.10 | Si ⁴⁺ | 1.10 | 0.096 |
| SnO | 13.48 | 6.8 | 134.709 | 0.50 | O ²⁻ | 7.62 | 0.667 |
| MnCO ₃ | 3.95 | 1.7 | 114.9469 | 0.15 | Sn ²⁺ | 0.5 | 0.044 |
| NH ₄ Br | 13.36 | 49 | 97.94 | 0.5 | Mn ²⁺ | 0.15 | 0.013 |

2.2. Simulation of TRP

To simulate the RP-WLEDs with the remote phosphor structure having the ACCTs of 8500 K, 7700 K, 7000 K, 6600 K, and 5600 K, the LightTools 8.1.0 software, which is based on the Monte Carlo ray-tracing method, is applied. In Figure 1, the physical model of WLEDs is simulated in the 3-D form to illustrate the optical simulations of remote package WLEDs. This model is constructed with a reflector, a remote phosphor layer, and a package of 9 LED chips. Specifically, the reflector is designed with the length of 8 mm and 9.85 mm for the bottom and top surfaces, respectively, while its height is 2.07 mm. In addition, the remote phosphor layer covers the package of LED chips with the thickness fixed at 0.08 mm. Each LED chip has a 1.14 mm square base and a height of 0.15 mm. Moreover, these LED chips are bound in the cavity of the reflector. Besides, each blue chip is set with the radiant flux of 1.16 W at wavelength 455 nm. While the concentration range of phosphor grains fluctuates from 2% to 24%. Meanwhile, the ACCTs are maintained stable by controlling YAG:Ce³⁺ wt.



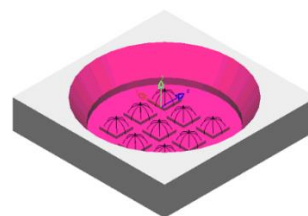
Lead frame: 4.7 mm Jentech Size-S
LED chip: V45H
Die attach: Sumitomo 1295SA
Gold Wire: 1.0 mil
Phosphor: ITC NYAG4_EL

(a)

(b)



(c)



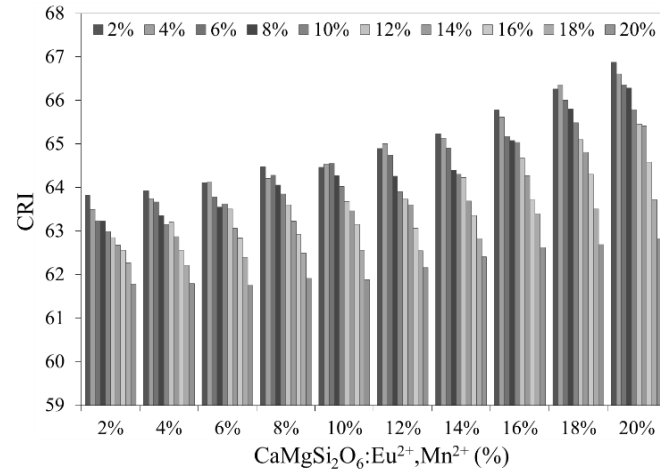
(d)

Figure 1. (a) WLEDs, (b) its parameters, (c) Illustration of triple-layer remote phosphor configuration, (d) the simulation of WLEDs

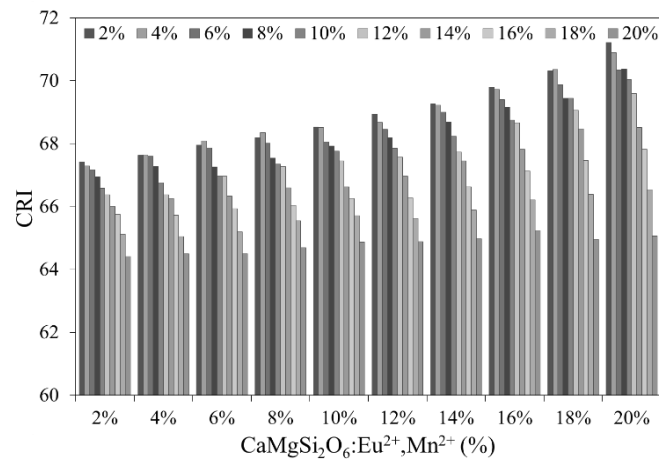
3. Results and Analysis

Figure 2 illustrated different values of CRI accompanying with the increase from 2% to 20% of red and green phosphor concentrations. As can be seen, CRI gradually increased in connection with the additional red phosphor concentration and reached the maximum value at the concentration of 20%. Conversely, the increase in green phosphor was not beneficial to CRI. The evidence was that when the green phosphor grew from 2% to 20%, there was a gradual decline in CRI regardless of the increase in red phosphor or the change in average correlated color temperature (ACCT). From the results in Figure 2, it can be affirmed that the red light components in WLEDs, which are produced from the red $\text{CaMgSi}_2\text{O}_6:\text{Eu}^{2+},\text{Mn}^{2+}$ phosphor layer, need to be increased to raise the CRI value. When there is a rise in the green phosphor concentration of $\text{Ba}_2\text{Li}_2\text{Si}_2\text{O}_7:\text{Sn}^{2+},\text{Mn}^{2+}$, the green light component will gain dominance; but this will not be advantageous to CRI. Moreover, the converted energy in the red phosphor layer declines when the green phosphor concentration rises. According to the TRP structure, the green phosphor layer lays underneath the red phosphor one, and this means that the light will reach the red phosphor first, before going through the green phosphor. Therefore, the green $\text{Ba}_2\text{Li}_2\text{Si}_2\text{O}_7:\text{Sn}^{2+},\text{Mn}^{2+}$ phosphor concentration should be chosen at the minimum value if the goal is the CRI enhancement. However, CRI is just one of the factors used to evaluate the color quality of WLEDs. It shows the ability of recognizing the true color of an object of human eyes when the light is shining. Besides the true color of the object, the viewer's preference and the color coordinates are the two important elements that the CRI cannot evaluate. Thus, color quality scale (CQS) can have the overall evaluation of the three factors: the CRI, the viewer's preference and the color coordinates of white lights. Hence, compared to CRI, CQS is more vital and difficult to achieve. Nonetheless, there is a raised question about how to improve the CQS value of WLEDs. Does it just simply increase the red light component as same as the way to enhance CRI? To figure out the answers for these questions, the value of CQS is shown as in Figure 3. Generally, CQS also grows up as the red $\text{CaMgSi}_2\text{O}_6:\text{Eu}^{2+},\text{Mn}^{2+}$ phosphor concentration increases. Nevertheless, unlike CRI, CQS presents a small difference when the concentration of green $\text{Ba}_2\text{Li}_2\text{Si}_2\text{O}_7:\text{Sn}^{2+},\text{Mn}^{2+}$ phosphor changes. It can be concluded from the results of Figure 3 that both green and red phosphor can contribute to lifting the CQS. In addition, the balance among the three principal colors: yellow, green and red is the key to promote CQS. When the concentration of red or green phosphor increases, that of the yellow phosphor needs to be decreased to maintain the ACCT.

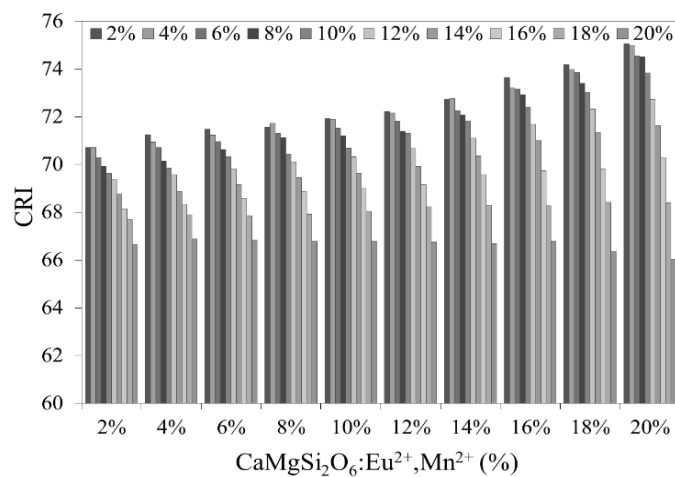
A decrease in the yellow phosphor concentration means that the yellow light component is declined, which brings WLEDs two benefits. One benefit is reducing the back-scattering event of lights to the chip LED so that the emitted luminous flux could considerably go up. The other one is the yellow light components in WLEDs will be declined and therefore is prevailed by the red and green light components. Moreover, managing CQS means controlling these three-color components. Besides, the CQS gradually increases when lifting the concentration of green $\text{Ba}_2\text{Li}_2\text{Si}_2\text{O}_7:\text{Sn}^{2+},\text{Mn}^{2+}$ phosphor from 2% to 10%, and then decreases. The CQS reach the highest value in terms of the concentration range of $\text{Ba}_2\text{Li}_2\text{Si}_2\text{O}_7:\text{Sn}^{2+},\text{Mn}^{2+}$ from 10% to 14%. When the green phosphor concentration is low, from 2% to 10%, the yellow light components still have most of the advantages. Moreover, there is a loss in the energy of light transmission causing the CQS cannot reach the maximum. While, as the concentration of the green phosphor is in the range from 10% to 14%, the green light components will be sufficient to get the CQS achieved the highest. However, when $\text{Ba}_2\text{Li}_2\text{Si}_2\text{O}_7:\text{Sn}^{2+},\text{Mn}^{2+}$ concentration rises over this range, the green light will be excessive leading to the imbalance among the three principle color green, red and yellow. Hence, the more the green phosphor concentration is raised, the more the CQS decreases. Controlling the color quality using the remote phosphor structure is more complex, compared to the two other structures conformal phosphor and in-cup phosphor. Moreover, in terms of the WLEDs with high ACCTs from 7000 K to 8500 K, this is more difficult to achieve. Nonetheless, the results show that with the TRP structure, the higher the ACCTs, the larger the CQS. In addition, not only reducing the back-scattering lights but the TRP structure also supports to increase the scattering lights inside WLEDs. This scattering enhancement means the process of mixing the light components is advanced, resulting in generating the white light with better quality. However, does this enhancement of the scattering process cause the transmitted light power to decline.



(a)

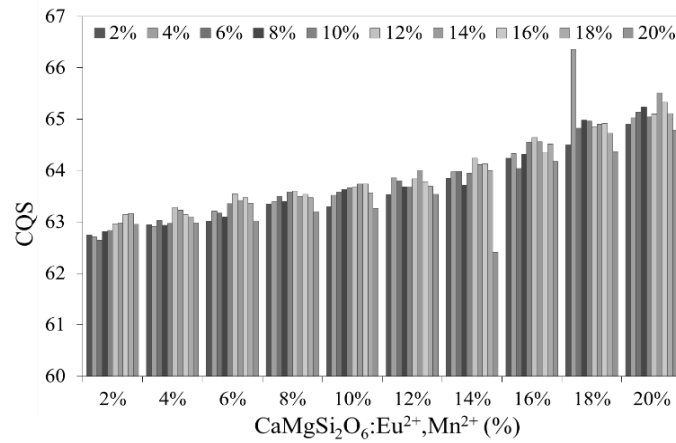


(b)

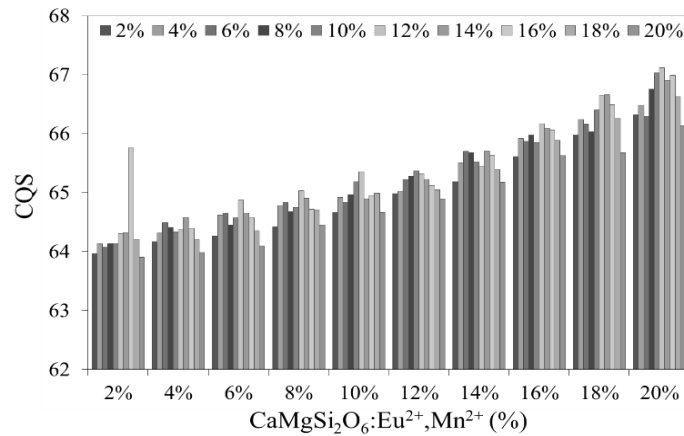


(c)

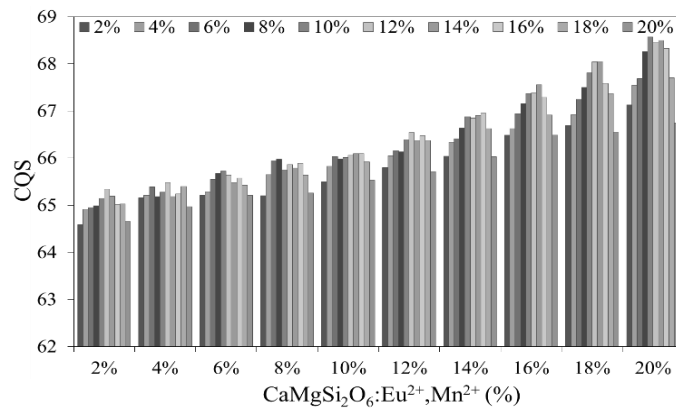
Figure 2. CRI of TRP as a function of red $\text{CaMgSi}_2\text{O}_6:\text{Eu}^{2+}, \text{Mn}^{2+}$ phosphor và green $\text{Ba}_2\text{Li}_2\text{Si}_2\text{O}_7:\text{Sn}^{2+}, \text{Mn}^{2+}$ phosphor: (a) 6000 K (b) 7000 K (c) 8500 K



(a)



(b)



(c)

Figure 3. CQS of TRP as a function of red $\text{CaMgSi}_2\text{O}_6:\text{Eu}^{2+},\text{Mn}^{2+}$ phosphor và green $\text{Ba}_2\text{Li}_2\text{Si}_2\text{O}_7:\text{Sn}^{2+},\text{Mn}^{2+}$ phosphor: (a) 6000 K (b) 7000 K (c) 8500 K

In this part, there will be the mathematical model of the transmitted blue light and converted yellow light in the double-layer phosphor structure that results in a huge enhancement of LED efficiency. Moreover, these formulas are also demonstrated in this part. The transmitted

blue light and converted yellow light for single layer remote phosphor package with the phosphor layer thickness of $2h$ are shown in the following expressions [21-25]:

$$PB_1 = PB_0 \times e^{-2\alpha_{B1}h} \quad (1)$$

$$PY_1 = \frac{1}{2} \frac{\beta_1 \times PB_0}{\alpha_{B1} - \alpha_{Y1}} (e^{-2\alpha_{Y1}h} - e^{-2\alpha_{B1}h}) \quad (2)$$

The (3) and (4) formulas below present the transmitted blue light and converted yellow light for double layer remote phosphor package with the phosphor layer thickness of h :

$$PB_2 = PB_0 \times e^{-2\alpha_{B2}h} \quad (3)$$

$$PY_2 = \frac{1}{2} \frac{\beta_2 \times PB_0}{\alpha_{B2} - \alpha_{Y2}} (e^{-2\alpha_{Y2}h} - e^{-2\alpha_{B2}h}) \quad (4)$$

In these equations, the thickness of each phosphor layer is expressed as h . The subscript "1" and "2" are used to describe single layer and double-layer remote phosphor package. β presents the conversion coefficient for blue light converting to yellow light. γ is the reflection coefficient of the yellow light. The intensities of blue light (PB) and yellow light (PY) are the light intensity from blue LED, indicated by PB_0 . α_B ; α_Y are parameters describing the fractions of the energy loss of blue and yellow lights during their propagation in the phosphor layer respectively. The lighting efficiency of pc-LEDs with the double-layer phosphor structure significantly promoted when compared to a single layer structure:

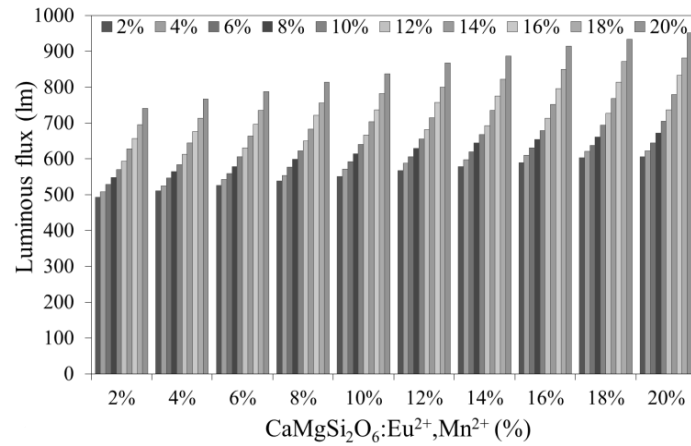
$$\frac{(PB_2 + PY_2) - (PB_1 + PY_1)}{PB_1 + PY_1} > 0 \quad (5)$$

Additionally, the Mie-theory is applied to analyze the scattering of phosphor particles. Besides, based on Mie-theory, the scattering cross section C_{sca} for spherical particles can be calculated by the following expression. The transmitted light power can be calculated by the Lambert-Beer law:

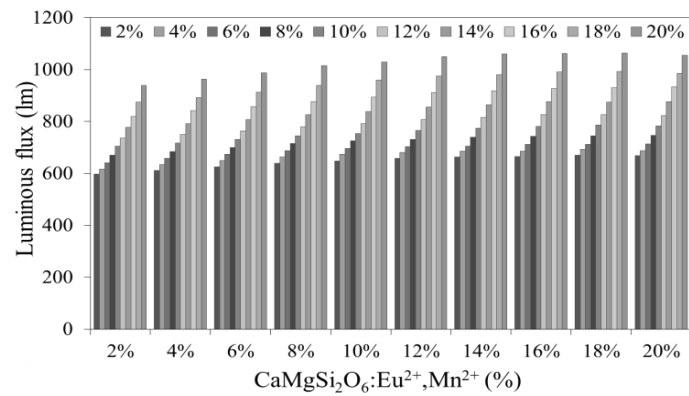
$$I = I_0 \exp(-\mu_{ext}L) \quad (6)$$

In this formula, I_0 is the incident light power, L is the phosphor layer thickness (mm) and μ_{ext} is the extinction coefficient, which can be expressed as: $\mu_{ext} = N_r \cdot C_{ext}$, where N_r presents the number density distribution of particles (mm^{-3}). C_{ext} (mm^2) indicates the extinction cross-section of phosphor particles. The (5) proves that using the additional phosphor layer can heighten the emitted luminous flux of WLEDs. The luminous flux increases as a result of the growth in the red and green phosphor concentrations. In order to remain the ACCTs when the concentrations of the red and green phosphor go up, the yellow light concentration has to be reduced. Additionally, the key point in reducing the yellow light concentration is to have light energy generating from the back-scattering event decreased. Moreover, the decline in the concentration of yellow phosphor contributes to the greater transmitted light power, according to the Lambert-Beer law in (6). Therefore, the higher the concentration of $\text{Ba}_2\text{Li}_2\text{Si}_2\text{O}_7:\text{Sn}^{2+}, \text{Mn}^{2+}$ or $\text{CaMgSi}_2\text{O}_6:\text{Eu}^{2+}, \text{Mn}^{2+}$ phosphor layer, the greater the luminous flux is emitted. Nevertheless, this result is not beneficial to CQS. The excess red or green light components cause the color imbalance resulting in the decline of CQS.

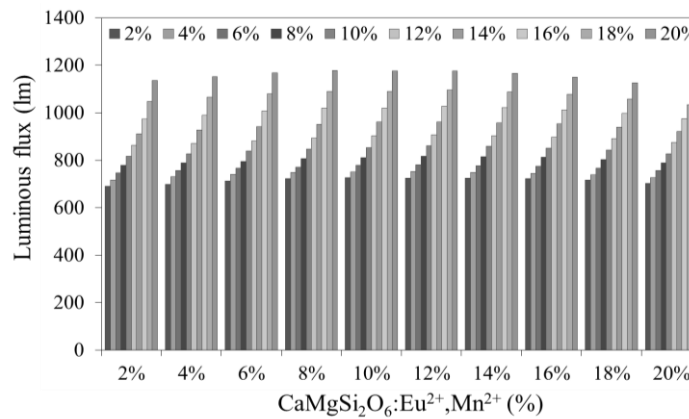
According to the results from Figure 4, the phosphor layer of $\text{Ba}_2\text{Li}_2\text{Si}_2\text{O}_7:\text{Sn}^{2+}, \text{Mn}^{2+}$ can get the luminous efficacy (LE) risen over 40%, regardless of the $\text{CaMgSi}_2\text{O}_6:\text{Eu}^{2+}, \text{Mn}^{2+}$ phosphor concentration, due to the increase of green light components and the decrease of lights from back-scattering. The obtained results are valuable references for manufacturers to easily choose the appropriate amount for the concentration of these two phosphors. Specifically, to achieve the highest range of value for CQS and LE, the concentration of $\text{Ba}_2\text{Li}_2\text{Si}_2\text{O}_7:\text{Sn}^{2+}, \text{Mn}^{2+}$ and $\text{CaMgSi}_2\text{O}_6:\text{Eu}^{2+}, \text{Mn}^{2+}$ should be selected from 10% to 14% and at 20%, respectively. While LE also slightly increases with the presence of $\text{CaMgSi}_2\text{O}_6:\text{Eu}^{2+}, \text{Mn}^{2+}$ concentration at ACTTs 6000 K and 7000 K. At ACCT 8500 K, LE is almost unchanged in the concentration range from 2% to 14% of $\text{CaMgSi}_2\text{O}_6:\text{Eu}^{2+}, \text{Mn}^{2+}$. Then LE shows a slight decrease when the green phosphor concentration is raised to 20%.



(a)



(b)



(c)

Figure 4. Luminous flux of TRP as a function of red $\text{CaMgSi}_2\text{O}_6:\text{Eu}^{2+},\text{Mn}^{2+}$ phosphor và green $\text{Ba}_2\text{Li}_2\text{Si}_2\text{O}_7:\text{Sn}^{2+},\text{Mn}^{2+}$ phosphor: (a) 6000 K (b) 7000 K (c) 8500 K

4. Conclusion

The TRP structure with two phosphor layers of $\text{Ba}_2\text{Li}_2\text{Si}_2\text{O}_7:\text{Sn}^{2+},\text{Mn}^{2+}$ and $\text{CaMgSi}_2\text{O}_6:\text{Eu}^{2+},\text{Mn}^{2+}$ is proposed to enhance CRI, CQS, and LE of WLEDs. Not only does

the TRP structure get the color quality promoted, but also the LE, which is a new result that has not been attained before. In order to achieve these results, it is essential to get the three yellow, red and green lights in the phosphor layer balanced through managing the concentration of $\text{Ba}_2\text{Li}_2\text{Si}_2\text{O}_7:\text{Sn}^{2+},\text{Mn}^{2+}$ and $\text{MgSi}_2\text{O}_6:\text{Eu}^{2+},\text{Mn}^{2+}$. Specifically, controlling the green $\text{Ba}_2\text{Li}_2\text{Si}_2\text{O}_7:\text{Sn}^{2+},\text{Mn}^{2+}$ phosphor layer is managing the green light component inside WLEDs, resulting in the luminous flux increasing. Furthermore, the application of an additional phosphor layer is more beneficial to luminous efficiency than using only one layer. Besides, managing the concentration of the red $\text{CaMgSi}_2\text{O}_6:\text{Eu}^{2+},\text{Mn}^{2+}$ phosphor layer means manipulating the red light component inside WLEDs, leading to the growth in CRI. Additionally, the researched results present that the balance among the three colors: yellow, green and red, and the reduction in back-scattering from yellow $\text{YAG}:\text{Ce}^{3+}$ will bring the highest color quality and luminous flux of WLEDs.

References

- [1] Li CN, Rao HB, Zhang W, Zhou CY, Zhang Q, Zhang K. Self-Adaptive Conformal-Remote Phosphor Coating of Phosphor-Converted White Light Emitting Diodes. *Journal of Display Technology*. 2016; 12(9): 946-950.
- [2] NDQ, Le PX, Lee HY. Selection of a Remote Phosphor Configuration to Enhance the Color Quality of White LEDs. *Current Optics and Photonics*. 2019; 3(1): 78-85.
- [3] Li ZT, Wang HY, Yu BH, Ding XR, Tang Y. High-efficiency LED COB device combined diced V-shaped pattern and remote phosphor. *Chinese Optics Letters*. 2017; 15(4).
- [4] Ying SP, Shen JY. Concentric ring phosphor geometry on the luminous efficiency of white-light-emitting diodes with excellent color rendering property. *Optics Letters*. 2016 4 (9): 1989-1992.
- [5] Chiang CH, Tsai HY, Zhan TS, Lin HY, Fang YC, Chu SY. Effects of phosphor distribution and step-index remote configuration on the performance of white light-emitting diodes. *Optics Letters*. 2015; 40(12): 2830-2833.
- [6] Yu SD, Li ZT, Liang GW, Tang Y, Yu BH, Chen KH. Angular color uniformity enhancement of white light-emitting diodes by remote micro-patterned phosphor film. *Photonics Research*. 2016; 4(4): 140-145.
- [7] Jeon SW, Kim SH, Choi JN, Jang IS, Song YH, Kim WH, Kim JP. Optical design of dental light using a remote phosphor light-emitting diode package for improving illumination uniformity. *Applied Optics*. 2018; 5 (21): 5998-6003.
- [8] Xie B, Chen W, Hao JN, Wu D, Yu XJ, Chen YH, Hu R, Wang K, Luo XB. Structural optimization for remote white light-emitting diodes with quantum dots and phosphor: packaging sequence matters. *Optics Express*. 2016; 24(26): A1560-A1570.
- [9] Li JS, Li ZT, Liang GW, Yu SD, Tang Y, Ding XR. Color uniformity enhancement for COB WLEDs using a remote phosphor film with two freeform surfaces. *Optics Express*. 2016; 24(21): 23685-23696.
- [10] Shih BJ, Chiou SC, Hsieh YH, Sun CC, Yang TH, Chen SY, Chung TY. Study of temperature distributions in pc-WLEDs with different phosphor packages. *Optics Express*. 2015; 23(26): 33861-33869.
- [11] Guo ZQ, Lu HL, Shih TM, Lin Y, Lu YJ, Chen Z. Spectral Optimization of Candle-Like White Light-Emitting Diodes With High Color Rendering Index and Luminous Efficacy. *Journal of Display Technology*. 2016; 12(11): 1393-1397.
- [12] Ran Ma R, Chaoyang Ma CY, Jiantao Zhang JT, Jiaqi Long JQ, Zicheng Wen ZC, Xuanyi Yuan XY, and Yongge Cao YG. Energy transfer properties and enhanced color rendering index of chromaticity tunable green-yellow-red-emitting $\text{Y}_3\text{Al}_5\text{O}_{12}:\text{Ce}^{3+},\text{Cr}^{3+}$ phosphors for white light-emitting diodes. *Optical Materials Express*. 2017; 7(2): 454-467.
- [13] Anh NDQ, Vinh NH, Lee HY. Effect of Red-emitting $\text{Sr}_{2.41}\text{F}_{2.59}\text{B}_{20.03}\text{O}_{74.8}:\text{Eu}_{0.12},\text{Sm}_{0.048}$ Phosphor on Color Rendering Index and Luminous Efficacy of White LEDs. *Current Optics and Photonics*. 2017; 1(2): 118-124.
- [14] Li NQ, Zhang Y, Quan YW, Li L, Ye SH, Fan QL, Huang W. High-efficiency solution-processed WOLEDs with very high color rendering index based on a macrospirocyclic oligomer matrix host. *Optical Materials Express*. 2018; 8(10): 3208-3219.
- [15] Li YY, Chen JJ, Feng HH, Chen H, Wang QM. Rugate filters used in slit-lamp delivery to improve color rendering of illumination for retinal photocoagulation. *Applied Optics*. 2014; 53(15): 3361-3369.
- [16] Yiyu Ou YY, Corell DD, Dam-Hansen C, Petersen PM, Ou HY. Antireflective sub-wavelength structures for improvement of the extraction efficiency and color rendering index of monolithic white light-emitting diode. *Optics Express*. 2011; 19(S2): A166-A172.
- [17] He GX GX, Tang J. Study on the correlations between color rendering indices and the spectral power distributions: comment. *Optics Express*. 2015; 23(3): A140-A145.

- [18] Hung PC, Tsao JY. Maximum White Luminous Efficacy of Radiation Versus Color Rendering Index and Color Temperature: Exact Results and a Useful Analytic Expression. *Journal of Display Technology*. 2013; 9(6): 405-412.
- [19] Huyal IO, Ozel T, Koldemir U, Nizamoglu S, Tuncel D, Demir HV. White emitting polyfluorene functionalized with azide hybridized on near-UV light emitting diode for high color rendering index. *Optics Express*. 2008; 16(2): 1115-1124.
- [20] Erdem T, Nizamoglu S, Sun XW, Demir HV. A photometric investigation of ultra-efficient LEDs with high color rendering index and high luminous efficacy employing nanocrystal quantum dot luminophores. *Optics Express*. 2010; 18(1): 340-347.
- [21] Yan QR, Zhang Y, Li ST, Yan QA, Shi PP, Niu QL, He MA, Li GP, Li JR. Improved color rendering of phosphor-converted white light-emitting diodes with dual-blue active layers and n-type AlGaN layer. *Optics Letters*. 2012; 37(9): 1556-1558.
- [22] Jost S, Cauwerts C, Avouac P. CIE 2017 color fidelity index Rf: a better index to predict perceived color difference?. *Journal of the Optical Society of America A*. 2018; 35(4): B202-B213.
- [23] Ying SP, Fu HK, Hsieh HH, Hsieh KY. Color design model of high color rendering index white-light LED module. *Applied Optics*. 2017; 56(14): 4045-4051.
- [24] Wang L, Zhang X, Hao ZD, Luo YS, Wang XJ, Zhang JH. Enriching red emission of $Y_3Al_5O_{12}: Ce^{3+}$ by codoping Pr^{3+} and Cr^{3+} for improving color rendering of white LEDs. *Optics Express*. 2010; 18(24): 25177-25182.
- [25] David A, Fini PT, Houser KW, Ohno Y, Royer MP, Smet KAG, Wei M, Whitehead L. Development of the IES method for evaluating the color rendition of light sources. *Optics Express*. 2015; 23(12): 15888-15906.